

## Supporting Information

### Phytic Acid Cross-linked and Hoffmeister effect Strengthened Polyvinyl Alcohol Hydrogels for Zinc Ion Storage

Xinlong Liu<sup>a,c,#</sup>, Yulin Cao<sup>a,c,#</sup>, Haiou Wang<sup>c</sup>, Yingqi Hu<sup>c</sup>, Zhan Wang<sup>c</sup>, Yingzhi Li<sup>c</sup>,  
Weimin Yang<sup>a,\*</sup>, Hua Cheng<sup>b,\*</sup>, Zhouguang Lu<sup>c,\*</sup>

a. Industrial Training Center, Shenzhen Polytechnic University, Shenzhen 518055,  
Guangdong, P. R. China.

b. School of Materials Science and Environmental Engineering, Shenzhen  
Polytechnic University, Shenzhen 518055, Guangdong, P. R. China.

c. Department of Materials Science and Engineering, Southern University of  
Science  
and Technology, Shenzhen, 518055, P. R. China.

\* E-mail: ywm13@163.com (W.M. Yang); chenghua@szpt.edu.cn (H. Cheng);  
luzg@sustech.edu.cn (Z.G. Lu)

# These two authors contributed equally to this work.

## **Experimental**

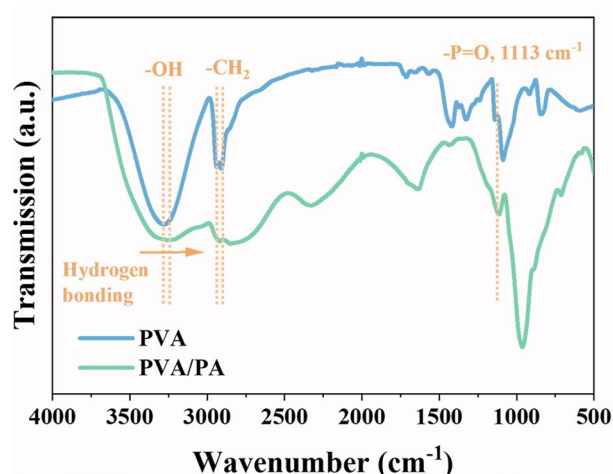
### **Preparation of hydrogels**

The PVA/PA hydrogels were synthesized via simple freeze/thaw process. In detail, 10 wt% transparent PVA solution was firstly prepared by adding PVA (M.W. 105000) into phytic solution (50 wt%) with continuous stirring for 4 h. After transferred to a plastic moule overnight, the sticky solution was stored in a refrigerator at -25 °C for 2 h and then stand for 2 h at ambient temperature. The above freeze/thaw procedure was repeated three times. Finally, the above hydrogel was immersed into 2.0 M ZnSO<sub>4</sub> solution for 2 h to yield PVA/PA flexible hydrogels.

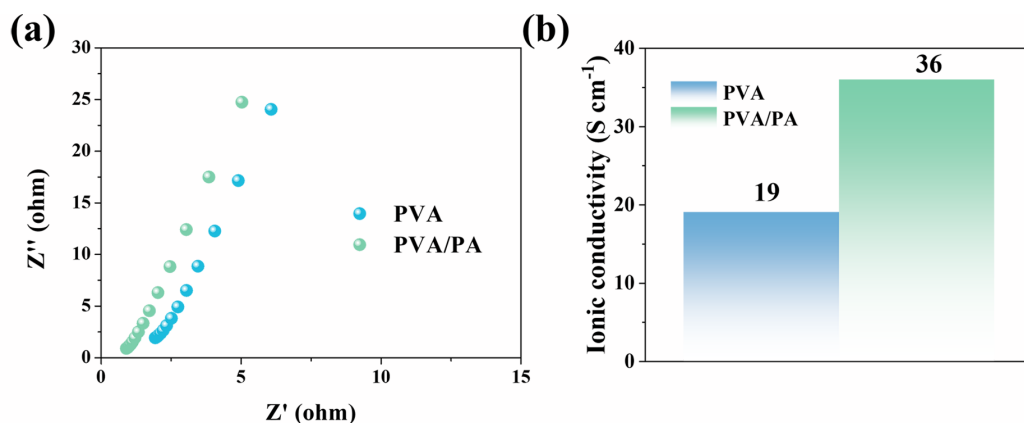
### **Materials characterizations and electrochemical measurements**

The morphologies of all hydrogels were observed by field emission transmission electron microscope (SEM). The crystal structure of MnO<sub>2</sub> nanorods was determined by X-ray diffractometer (XRD) with scanning angle from 5° to 80°. The zinc plate was polished before assembly in coincell. Zn||AC asymmetric or Zn||MnO<sub>2</sub> cells were assembled in CR2032 coin cells with Zn, glass fibers (GF/A), hydrogels electrolyte, and activated carbon or MnO<sub>2</sub> cathode (Aladdin, 99%, metals basis). MnO<sub>2</sub> cathodes or AC electrode were fabricated by pasting 70% MnO<sub>2</sub> or AC, 20% carbon black, and 10% lithium polyacrylate (LiPAA) binder onto Ti foil. Electrochemical impedance spectroscopy (EIS), cyclic voltammetry (CV) and linear sweep voltammetry (LSV) measurements were performed on a CHI660E electrochemical workstation.

## Supporting Figures



**Fig. S1** FT-IR spectra of pure PVA and PVA/PA hydrogels <sup>1-2</sup>.



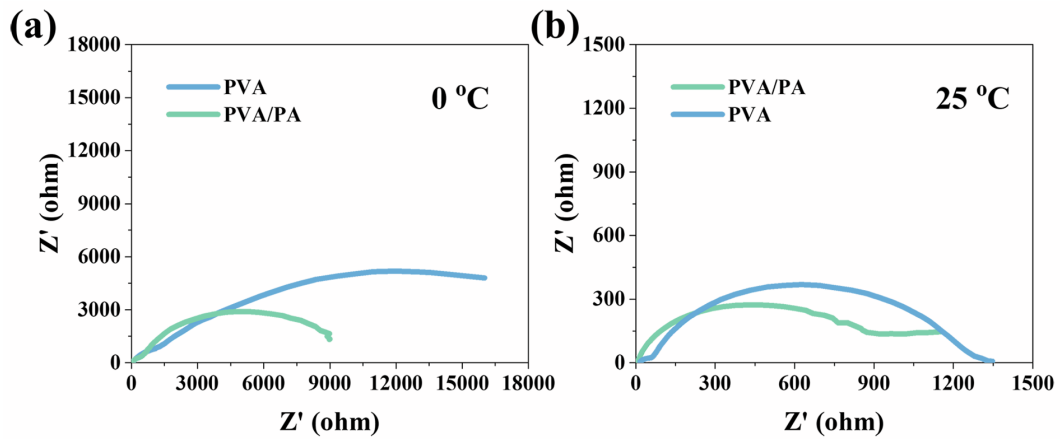


Fig. S3. EIS curves of PVA and PVA/PA hydrogel at room temperature and freezing point.

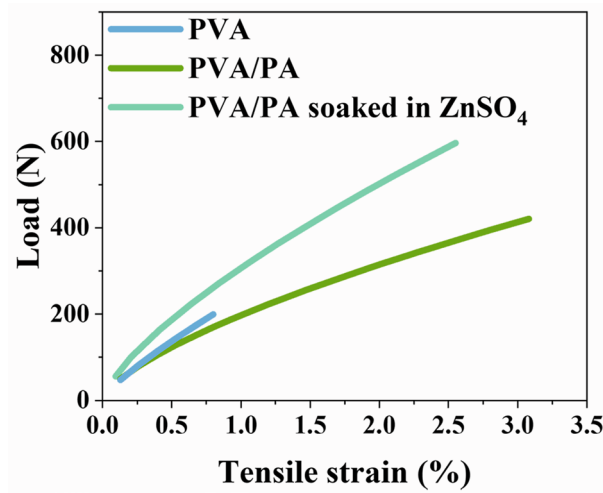


Fig. S4. Tensile strain of PVA, PVA/PA, and soaked PVA/PA hydrogels.

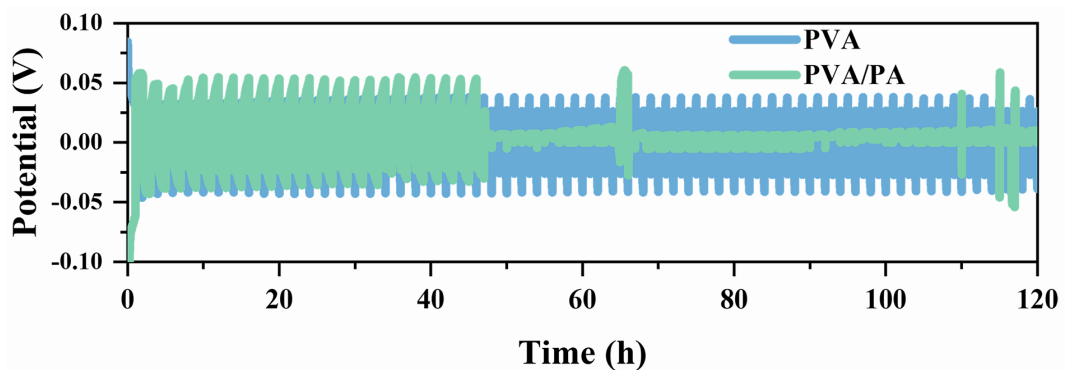
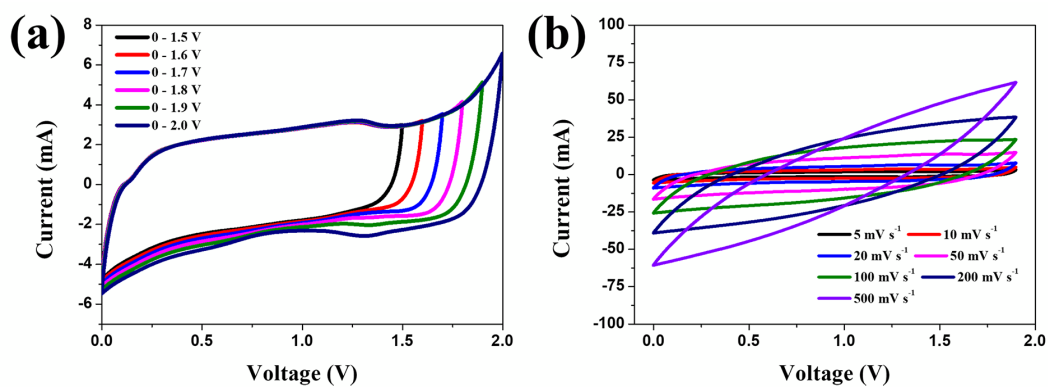
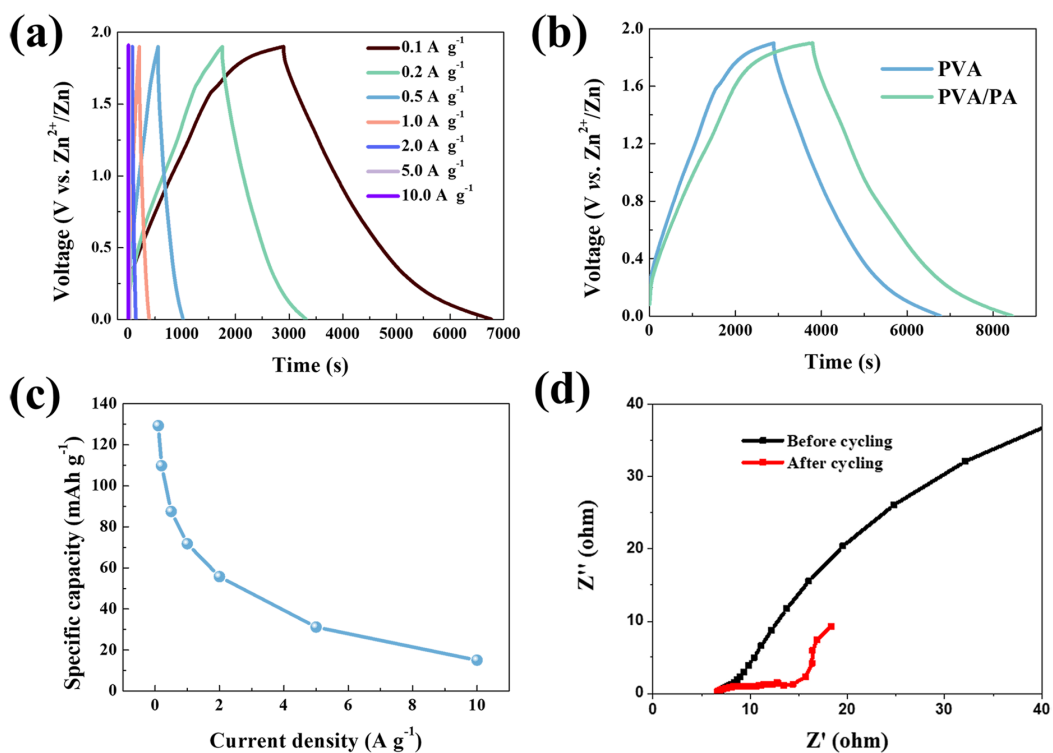


Fig. S5 Time-voltage curve for Zn||Zn cell of hydrogel electrolytes at 1.0 mA cm<sup>-2</sup>.



**Fig. S6.** a) CV curves in Zn|PVA/PA|AC asymmetric capacitor with scanning rate of 5.0 mV s<sup>-1</sup>; b) CV curves of Zn|AC capacitor at various scan rate.



**Fig. S7.** a) Galvanostatic charge/discharge profiles of PAV hydrogel; b) Comparison of charge/discharge profiles between PVA and PVA/PA hydrogels at 0.1 A g<sup>-1</sup>; c) Rate capability under different current densities. d) EIS curves of PVA/PA hydrogel before after cycling.

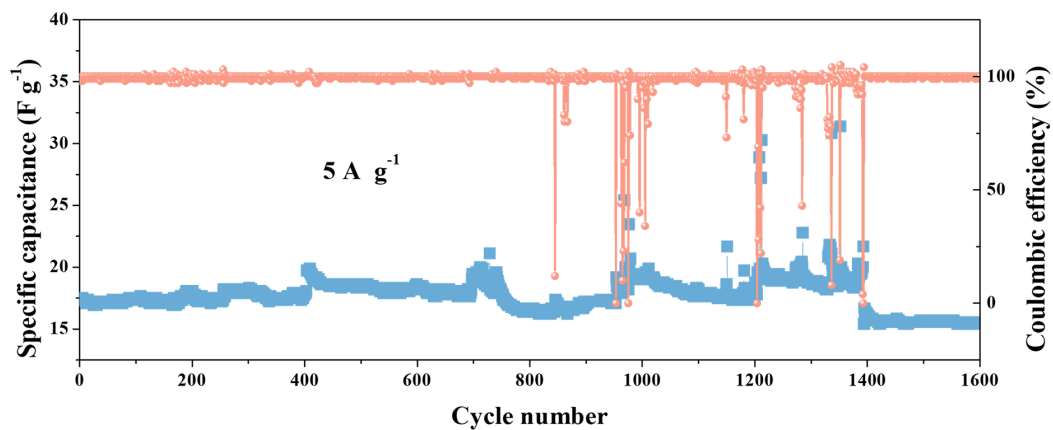


**Figure S8.** a) Cycling performance at a current density of  $5.0 \text{ A g}^{-1}$ .

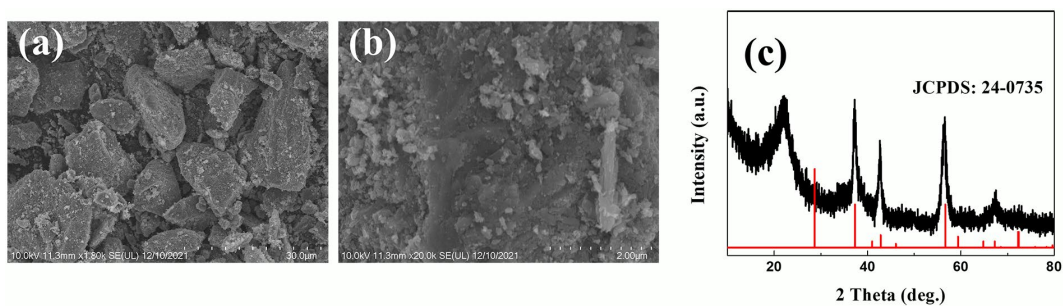


**Fig. S9.** a,b) SEM images of as synthesized  $\text{MnO}_2$  nanoparticles. c) XRD pattern of  $\text{MnO}_2$  nanoparticles.

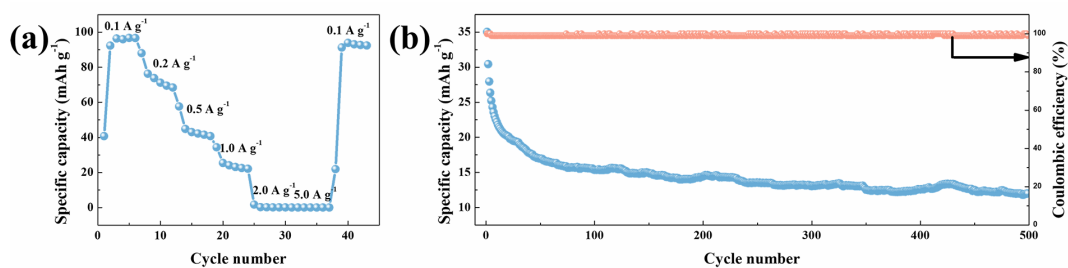


**Fig. S10.** a) Rate capability and b) cycling performance of PVA hydrogels.

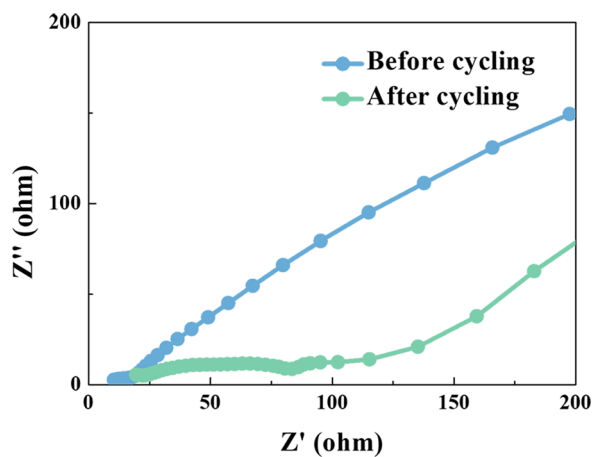


**Fig. S11.** EIS curve of PVA/PA hydrogels in battery before and after cycling.

**Table S1** Full-cell performance of MnO<sub>2</sub> cathodes among reported works.

MnO <sub>2</sub> cathode	Rate capability (A g <sup>-1</sup> , mAh g <sup>-1</sup> )						
	0.1	0.2	0.5	1.0	2.0	5.0	This work
C-MnO <sub>2</sub>	225	200	150	125	100	50	This work
	0.5	1.0	3.0	5.0	7.0		
N doped-MnO <sub>2</sub>	183.4	128.6	96.4	62.5	50.6		3
	0.2	0.5	1.0	2.0			
S doped-MnO <sub>2</sub>	324	311	262	205			4
	0.1	0.2	0.3	0.5	0.7	1.0	
Modified Beta- MnO <sub>2</sub>	~225	~200	~183	~160	~145	~105	5
	0.1	0.2	0.3	0.5	1.0	2.0	
Ag doped-MnO <sub>2</sub>	290	250	215	177	128	85	6
	0.1	0.15	0.2	0.3	0.5	1.0	
$\alpha$ -MnO <sub>2</sub>	~230	~190	~175	~150	~110	~50	7
	1.0	1.5	2.0	2.5	3.0	3.5	
Ag doped-MnO <sub>2</sub>	~128	~120	~100	~85	~60	~50	8

## Supporting References

1. Zhao, J., Lu, Y., Liu, Y., Liu, L., Yin, J., Sun, B., Wang, G. and Zhang, Y., *Nanomaterials*, 2023, **13**(3), 380.
2. L. Zeng, B. Liu, G. Gao, *Sci. China Mater.*, 202366, **10**, 4062-4070.
3. Y. Zhang, Y. Liu, Z. Liu, X. Wu, Y. Wen, H. Chen, X. Ni, G. Liu, J. Huang, S. Peng, *J. Energy Chem.*, 2022, **64**, 23-32.
4. Y. Zhao, P. Zhang, J. Liang, X. Xia, L. Ren, L. Song, W. Liu, X. Sun, *Energy Storage Mater.*, 2022, **47**, 424-433.
5. Y. Liao, H.C. Chen, C. Yang, R. Liu, Z. Peng, H. Cao, K. Wang, *Energy Storage Mater.*, 2022, **44**, 508-516.
6. Y. Liao, C. Yang, Q. Xu, W. Zhao, J. Zhao, K. Wang, H.-C. Chen, *Batteries*, 2022, **8**, 267.
7. Y., Chen, Z. Li, B. Li, Z. Zhang, J. Wei, B. Wang, Y. Huang, *ACS Appl. Energy Mater.*, 2023, **6**(6), 3329-3336.
8. X. Pu, X. Li, L. Wang, H. Maleki Kheimeh Sari, J. Li, Y. Xi, H. Shan, J. Wang, W. Li, X Liu, S. Wang, *ACS Appl. Mater. Interfaces*, 2022, **14**(18), 21159-21172.